

Miscibility, Crystallization, and Mechanical Properties of Poly(3-hydroxybutyrate-co-4-hydroxybutyrate)/Poly(butylene succinate) Blends

Wenfu Zhu, Xiaojuan Wang, Xianyu Chen, Kaitian Xu

Multidisciplinary Research Center, Shantou University, Shantou, Guangdong 515063, China

Received 18 December 2008; accepted 14 June 2009

DOI 10.1002/app.30965

Published online 19 August 2009 in Wiley InterScience (www.interscience.wiley.com).

ABSTRACT: Naturally amorphous biopolyester poly(3-hydroxybutyrate-co-4-hydroxybutyrate) (P3/4HB) containing 21 mol % of 4HB was blended with semi-crystal poly(butylene succinate) (PBS) with an aim to improve the properties of aliphatic polyesters. The effect of PBS contents on miscibility, thermal properties, crystallization kinetics, and mechanical property of the blends was evaluated by DSC, TGA, FTIR, wide-angle X-ray diffractometer (WAXD), Scanning Electron Microscope (SEM), and universal material testing machine. The thermal stability of P3/4HB was enhanced by blending with PBS. When

PBS content is less than 30 wt %, the two polymers show better miscibility and their crystallization trend was enhanced by each other. The optimum mechanical properties were observed at the 5–10 wt % PBS blends. However, when the PBS content is more than 30 wt %, phase inversion happened. And the two polymers give lower miscibility and poor mechanical properties. © 2009 Wiley Periodicals, Inc. *J Appl Polym Sci* 114: 3923–3931, 2009

Key words: biopolyester; blends; miscibility; crystallization; mechanical properties

INTRODUCTION

Increasing attention has been paid to microbial polyester in recent years due to its resources renewable, biodegradable and potential applications as environmental friendly polymers for agricultural, marine, and medical applications.¹ Produced by *Ralstonia eutropha*, *Alcaligenes latus*, and *Comamonas acidovorans*, poly(3-hydroxybutyrate-co-4-hydroxybutyrate) (P3/4HB) was fermented successfully from 4-hydroxybutyric and butyric acid.^{2,3} The physical property of P3/4HB is from semi-crystallization plastics to amorphous elastomers depending on the 4-hydroxybutyrate (4HB) content.⁴ As plastics, P3/4HB possesses fairly good processing property. But the thermal stability of P3/4HB is less than 250°C and needs to be improved. In addition, when P3/4HB was used as elastomers, it had very low tensile strength and limited elongation at break.⁵ Several modifications have been proposed to improve its mechanical properties, such as chemical modification and physical blending, in which physical blending is

preferred because of the easy, fast, and low-cost working techniques.^{6–9}

Produced in chemosynthetic way, however, poly(butylene succinate) (PBS) is a linear aliphatic biodegradable polyester synthesized by polycondensation of 1,4-butanediol and succinic acid. The crystal structure, crystallization, and melting behavior of PBS have been reported.^{10–16} The thermal property of PBS is fairly good with the decomposition of more than 350°C. The nonisothermal crystallization kinetics and melting behavior of PBS were studied.^{17,18} PBS was found to be miscible with many polymers, including poly(vinylidene fluoride), poly(vinylidene chloride-co-vinyl chloride), and poly(ethylene oxide) in the literature.^{19–22} On the other hand, PBS was found to be immiscible with some biodegradable polymers, including poly(hydroxybutyrate) (PHB) and poly(3-hydroxybutyrate-co-3-hydroxyvalerate) (PHBV).^{23,24}

Both P3/4HB and PBS have been produced in large industrial scale in the hope of becoming novel, resources renewable, and non-fossil based commodity polymers. The purpose of our investigation was to seek the possibility of improving the thermal and mechanical properties of P3/4HB via the blending with PBS. To our knowledge, this is the first time that PBS was used for improving P3/4HB properties. The results would be interesting to the polymer materials industrial community which is driving to develop new materials source.

Correspondence to: K. Xu (ktxu@stu.edu.cn).

Contract grant sponsor: Natural Science Foundation of China; contract grant number: 20474001.

Contract grant sponsor: National High Tech 863 Grant; contract grant number: 2006AA02Z242.

EXPERIMENTAL SECTION

Materials

P3/4HB ($M_n = 1.3 \times 10^6$, $M_w/M_n = 1.2$; 21 wt % 4HB content, estimated by GPC and NMR, respectively) was provided by Tianjin GreenBio Materials (Tianjin, China). PBS ($M_n = 5.2 \times 10^4$; $M_w/M_n = 1.33$) was provided by Anqing Hexing (Anqing, China). Both P3/4HB and PBS were industrial grade and used without further purification.

Preparation of the blend films

The P3/4HB/PBS blend films were prepared through the dissolution of 5 g of PBS and P3/4HB in 100 mL of chloroform, refluxing for 1 h, cooling, and casting onto a glass dish. After the evaporation of chloroform, the resultant films were dried in vacuum at 30°C for 2 days to a constant weight.

Differential scanning calorimetry

The thermal transitions of the blends were characterized by DSC performed on a TA Instruments Q100 (New Castle) with an autotool accessory and calibrated with indium. The sample was heated from -60 to 160°C at a heating rate of $10^\circ\text{C}/\text{min}$ under a nitrogen atmosphere (50 mL/min). After isothermal annealed at 160°C for 3 min, the molten sample was quenched to -60°C at a cooling rate of $60^\circ\text{C}/\text{min}$. Subsequently, the sample was again heated from -60 to 160°C at a heating rate of 5 or $10^\circ\text{C}/\text{min}$. The second heating round of the DSC curves was used to analyze the thermal properties. The glass transition temperature (T_g) was taken as the midpoint of the heat capacity change. The melting temperature (T_m) and melting enthalpy (ΔH_f) were determined from endothermal DSC peaks. In the presence of multiple endothermal peaks, the maximum peak temperature was taken to be T_m . The cold crystallization temperature (T_c) and cold crystallization enthalpy (ΔH_c) were determined from the corresponding exothermal DSC peaks.

The isothermal crystallization of P3/4HB/PBS blend from the melt was examined by the same TA Instrument Q100. The sample was melted at 140°C for 3 min to destroy any thermal history, cooled to the crystallization temperature (T_c) at a cooling rate of $60^\circ\text{C}/\text{min}$, and then maintained at the T_c until the crystallization was completed. All operations were performed under nitrogen purge, and sample weight varied between 2 and 4 mg. The exothermal traces were recorded for the data analysis.

Thermogravimetric analysis

TGA was performed on a TA Instrument Q50 instrument (New Castle) calibrated with indium. The

temperature was ramped at a heating rate of $10^\circ\text{C}/\text{min}$ under nitrogen atmosphere to a temperature well above the degradation temperature of the polymers (500°C).

Fourier transform infrared spectroscopy

Transmission infrared spectra were measured by Nicolet IR 200 (Thermo Electron) spectrophotometer. Blend film 3 mg was dissolved in 1 mL chloroform, coated on a KBr pellet and dried before use. All samples were carried out with 64 scans at a resolution of 1 cm^{-1} at room temperature.

Mechanical properties

Dumbbell-shaped samples of PHB-based films (thickness = 0.2–0.3 mm, base width 6–7 mm, base length 3–7 cm) were used for mechanical tests. The elongation at break, tensile strength, and Young's modulus of the tested samples were determined with a CMT 4204 universal testing machine (Sans, China) at room temperature at an extension rate of 5 mm/min.

Wide-angle x-ray diffraction

Wide-angle x-ray diffraction (WAXD) studies were carried out on a Bruker D8 ADVANCE diffractometer using Ni-filtered Cu K α radiation ($\lambda = 0.154\text{ nm}$). WAXD patterns were recorded in the 2θ range, 5 – 40° at a scan speed of $1.0^\circ/\text{min}$ at room temperature.

Scanning electron microscopy

A JEOL JSM-6360 LA (JEOL, Japan) instrument was used to study the surface morphology of the polymer films. Samples were prepared by vacuum drying overnight. Surface images were recorded after the samples were coated with a thin layer of gold.

RESULTS AND DISCUSSION

Thermal stability of P3/4HB/PBS blend

The thermal properties of P3/4HB/PBS were investigated by DSC and TGA. The results are summarized in Table I. The TGA curves of neat P3/4HB, neat PBS, and P3/4HB/PBS blends are shown in Figure 1. All the blend samples gave a two-stage thermal decomposition behavior, which is corresponding to the decomposition of P3/4HB and PBS components, respectively. With the increase of PBS content, the initial weight loss temperature increases obviously. The temperature at the 5% weight loss of the blend samples increased from 244°C of neat P3/4HB to 296°C of 80 wt % PBS blend (Table I). The large

TABLE I
Thermal Properties of Neat P3/4HB, Neat PBS, and P3/4HB/PBS Blends^a

PBS (wt %)	$T_{g,1}^b$ (°C)	$T_{g,2}^b$ (°C)	$T_{c,1}$ (°C)	$\Delta H_{c,1}$ (J/g)	$T_{c,2}$ (°C)	$\Delta H_{c,2}$ (J/g)	T_m (°C)	ΔH_f (J/g)	X_c (%)	T_d (5%) ^c (°C)
0	/ ^d	-10.3	/	/	/	/	/	/	/	244
5	-28.3	-14.9	40.1	6.4	/	/	112.4	4.2	42.0	247
10	-28.5	-11.0	58.5	2.4	89.9	0.02	112.9	7.8	39.0	250
20	-31.1	-11.7	44.2	9.4	89.8	0.9	112.8	16.3	40.6	254
30	-27.5	-12.5	42.3	2.5	94.5	2.1	113.3	25.8	43.0	260
40	-30.1	-10.4	/	/	94.2	3.0	113.4	31.1	38.9	269
60	-31.6	-11.3	/	/	93.7	8.3	113.3	44.5	37.1	284
80	-32.5	-12.2	/	/	93.4	10.6	113.2	63.4	39.6	296
100	-33.1	/	/	/	93.2	10.0	114.3	76.2	38.1	354

^a DSC data from second heat run at 10°C/min.

^b T_g from second heat run at heat rate 5°C/min.

^c Temperature at 5% weight loss of the samples determined by TGA.

^d Not detected.

scale increase of decomposition temperature would enhance the thermal stability of P3/4HB, and thus, widen the processing window of the polyester materials.

DSC analysis of neat PBS and P3/4HB/PBS blends

The miscibility, melting, and nonisothermal crystallization behavior of neat P3/4HB, neat PBS, and P3/4HB/PBS blends were studied with DSC (at 10°C/min, Fig. 2). Glass transition temperatures (T_g) of P3/4HB and PBS were -10.3°C and -33.1°C (at 5°C/min, Fig. 3). All of the blends gave two T_g s. The higher T_g is corresponding to the P3/4HB component, the lower one is corresponding to PBS component. The T_g values are listed in Table I. The two T_g reveal the phase separation in the blend systems, and the two components P3/4HB and PBS are not completely miscible. Although all the T_g values did not have much change compared with the T_g of

related neat P3/4HB and neat PBS, most of the blends still show somewhat T_g inner-shift effect, especially when the PBS was less than 30 wt %, the T_g of P3/4HB component of all blends decrease from -10.3°C to -14.9°C. And the T_g of PBS component increased from -33.1°C to -28.3°C when PBS content is 5 wt % (Fig. 3). All these results revealed that there is some degree of miscibility between PBS and P3/4HB, even though the miscibility might be low in some compositions. In the blends of PBS content ranged from 5 wt % to 30 wt %, the T_g inner-shift effect was more obvious. This exhibits that the two polymers have better miscibility at this composition blends.

The crystallization degree of PBS in the blends was calculated according to:

$$X_c = \Delta H_f / (w \cdot \Delta H_f^0) \quad (1)$$

on the basis of the melting enthalpy fusion of 100% crystalline PBS (200 J/g).¹⁵ Where ΔH_f is the melting

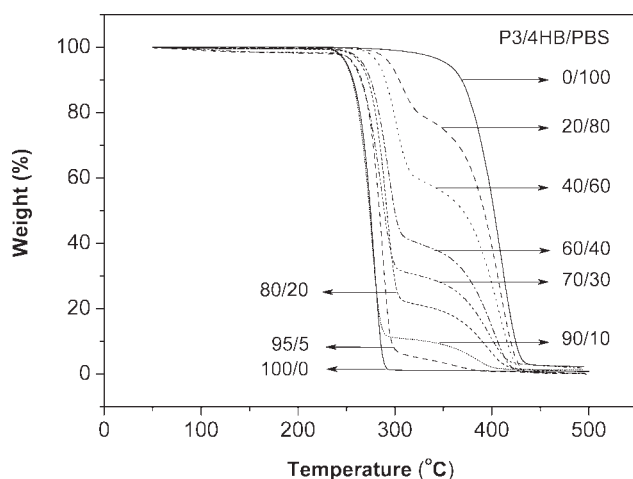


Figure 1 TGA curves of neat P3/4HB, neat PBS, and P3/4HB/PBS blends.

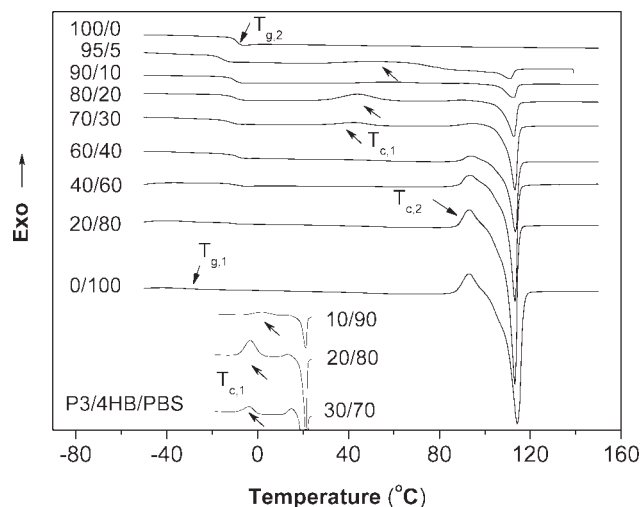


Figure 2 DSC thermograms of neat P3/4HB, neat PBS, and P3/4HB/PBS blends (second heat run, 10°C/min).

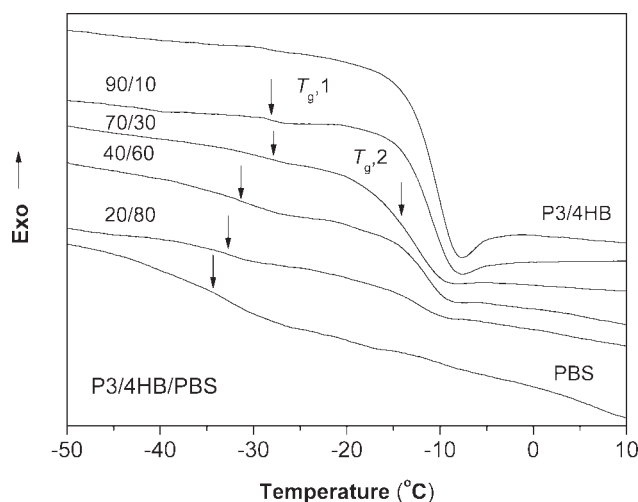


Figure 3 Glass transition temperature T_g for neat P3/4HB, neat PBS, and P3/4HB/PBS blends (second heat run, 5°C/min).

enthalpy of PBS in the blends, ΔH_f^0 is the melting enthalpy of 100% crystalline PBS, w is the weight fraction of PBS in the blends. The results of the crystallization degree of PBS in the blends are given in Table I. It was noted that in most of the blends, PBS shows the increase of crystallization degree more or less. In the case of P3/4HB/PBS (70/30) blend, the highest crystallization degree value which was about 5% higher than that of neat PBS was detected. It showed that the amorphous P3/4HB enhanced the crystallization of PBS.

All the blends showed a cold crystallization temperature at about 92°C (Fig. 2). The cold crystallization should be from the PBS component, as P3/4HB, if it is crystallizable, would give the cold crystallization temperature at around 50°C or less. When PBS was less than 30 wt %, the blends did, however, exhibit another broad cold crystallization temperature at round 40–60°C. The appearance of the cold crystallization at much lower temperature suggests that the crystallization of PBS probably enhanced the crystallization of P3/4HB as the nucleating agent. This result again revealed that stronger interaction happens and better miscibility was achieved between P3/4HB and PBS when the PBS content was less than 30 wt %.

The isothermal crystallization behaviors of P3/4HB/PBS blend

The isothermal crystallization behaviors of both neat PBS and P3/4HB/PBS blend are showed in Figure 4. The well-known Avrami equation was used to analyze the overall isothermal crystallization kinetics of both neat PBS and P3/4HB/PBS blend and the guidelines suggested by Müller were used to avoid common problems on the use of the Avrami

equation to fit the data.²⁵ It assumes that the relative degree of crystallinity X_t develops as a function of crystallization time t as follows:

$$1 - X_t = \exp(-kt^n)$$

$$\lg(-\ln(1 - X_t)) = \lg k + n \lg t \quad (2)$$

where X_t is the relative crystallinity at time t , k is the crystallization rate constant depending on nucleation and growth rate, and n is the Avrami exponent depending on the nature of nucleation and growth geometry of the crystals. Since determination of the absolute degree of crystallinity is not necessary in using Avrami analysis, the ratio of the area at time t and the area of whole exotherm was used to get X_t . Figure 4 shows the development of X_t as a function of crystallization time t for both neat PBS and P3/4HB/PBS (20/80) blend. It can be seen that the crystallization time increases with increasing crystallization temperature for both neat PBS and P3/4HB/

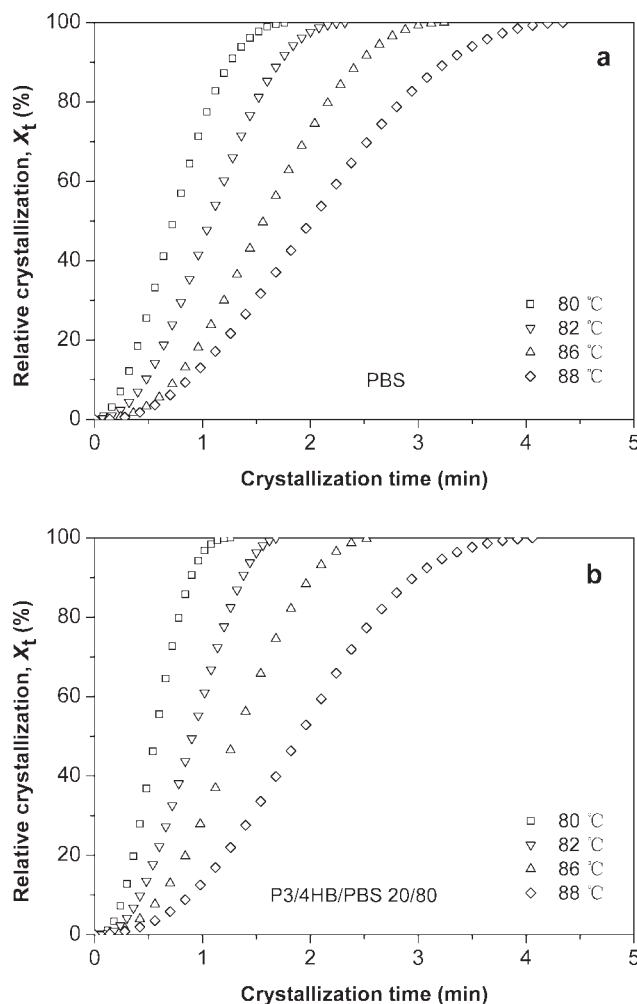


Figure 4 The plots of relative crystallinity X_t versus crystallization time t for (a) neat PBS and (b) P3/4HB/PBS (20/80) blend at different crystallization temperature.

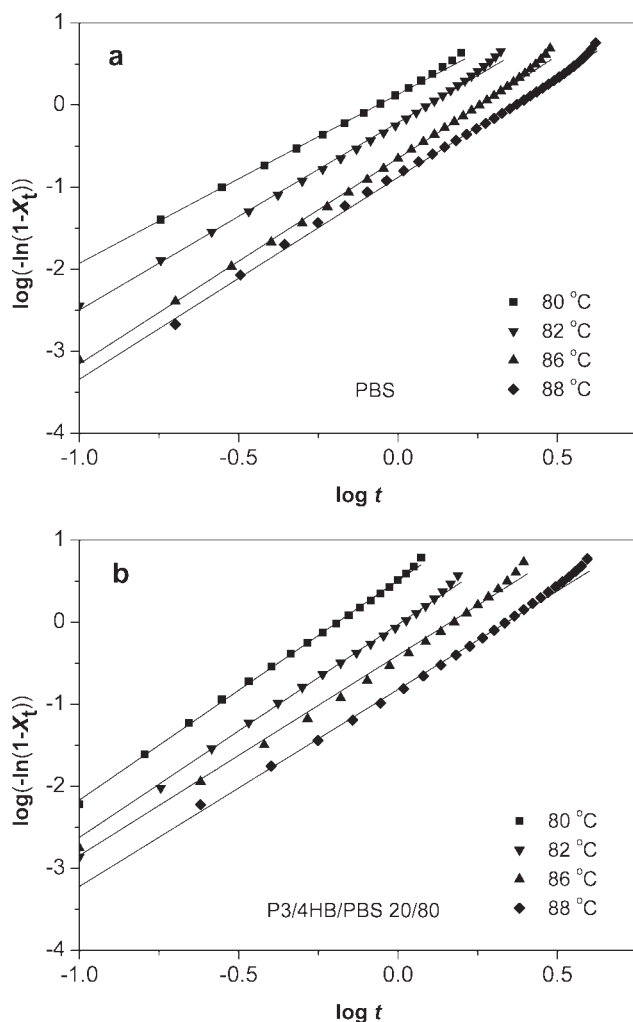


Figure 5 The Avrami plots of (a) neat PBS and (b) P3/4HB/PBS (20/80) blend at different crystallization temperature.

PBS blend, indicating that the crystallization was retarded with the increase of crystallization temperature. Compared with neat PBS, at a given crystallization temperature, however, the crystallization time of PBS component reduced when PBS was blended

with amorphous P3/4HB, indicating that the addition of amorphous P3/4HB increases the crystallization rate of PBS in the blend. The reason for the increase of crystallization rate of PBS in the blend will be discussed in the following section.

Figure 5 shows the Avrami plots for both neat PBS and P3/4HB/PBS blend. It was noted that the Avrami method can describe the development of relative crystallinity as a function of crystallization time quite well. Accordingly, the Avrami parameters n and k can be obtained from the slope and intercept respectively in the plots of $\log(-\ln(1 - X_t))$ versus $\log t$ as shown in Figure 5. The values of n and k are summarized in Table II, and the linear regression coefficient (R^2) was more than 0.995. The n value increases with increasing crystallization temperature and with the addition of P3/4HB component, indicating that the crystallization mechanism of PBS changes in the investigated crystallization temperature range as well as in the blend system. With increasing P3/4HB contents, the n value was elevated from 2.3 to 2.6, which suggested that the primary crystallization processes should correspond to a two-dimensional circular diffusion-controlled growth geometry and homogeneous nucleation ($n = 2$) or three-dimensional spherical growth ($n = 3$).²⁶ The increase of n value means complicated and larger crystal formed, as higher crystallization temperature would lead to less nucleation and higher single crystal growth rate due to the higher mobility of molecular chains. Moreover, the values of k decrease with increasing crystallization temperature for both neat PBS and P3/4HB/PBS blend, indicating that the overall crystallization rate is suppressed with the increase of crystallization temperature. On the other hand, the values of k increase with the addition of P3/4HB at the same crystallization temperature. Combining the also increase of n value with P3/4HB content, it further proved that the crystallization rate of PBS component was elevated with the addition of P3/4HB. The reason for the addition of P3/4HB increases the crystallization rate may be

TABLE II
The Isothermal Crystallization Kinetics Parameters for Neat PBS and P3/4HB/PBS (20/80) Blends at Different Crystallization Temperatures

	T_c (°C)	n	$k(\text{min}^{-n})$	Adj. R^2	$t_{0.5}$ (min) ^a	$\tau_{0.5}$ (min) ^b
PBS	88	2.5	0.13	0.9957	1.97	2.01
	86	2.5	0.22	0.9995	1.58	1.57
	82	2.3	0.61	0.9988	1.06	1.07
	80	2.1	1.29	0.9998	0.74	0.73
P3/4HB/PBS 20/80	88	2.4	0.15	0.9982	1.89	1.90
	86	2.5	0.33	0.9996	1.35	1.31
	82	2.6	0.94	0.9991	0.89	0.90
	80	2.7	3.25	0.9991	0.56	0.56

^a Predicted on n , k .

^b Calculated from Figure 4, $X_t = 0.5$.

TABLE III
Mechanical Properties of Neat P3/4HB
and P3/4HB/PBS Blend Films

PBS (wt %)	Tensile strength (MPa)	Elongation at break (%)	Young's modulus (MPa)
0	10.2	1145.8	53.9
5	16.3	1386.9	51.8
10	18.0	1355.1	85.3
20	11.7	942.6	109.2
30	4.0	17.5	136.2
40	7.8	77.4	197.4

related to the amorphous morphology of P3/4HB, which would supply more free space for the system. The free space would enhance the mobility of PBS chains and thus increase the crystallization rate. This effect also results in the increase of crystallinity X_c as indicated in Table I.

The half-life crystallization time $t_{0.5}$, which is defined as the time at $X_t = 0.5$, is an important parameter for the discussion of crystallization kinetics. It can also be calculated using the relation:

$$t_{0.5} = \left(\frac{\ln 2}{k} \right)^{1/n} \quad (3)$$

Usually, the crystallization rate can also be described as the reciprocal of $t_{0.5}$. $\tau_{0.5}$ is the experimental half-crystallization time, i.e., the time of $X_t = 0.5$, however, measured from Figure 4. By using the data listed in Table II and the aforementioned two equations, the values of $t_{0.5}$ and $\tau_{0.5}$ were obtained as a function of crystallization temperature and blend composition. It can be seen from Table II that the value of $t_{0.5}$ increases for both neat PBS and P3/4HB/PBS blend with the increase of the crystallization temperature. The value of $t_{0.5}$ for neat PBS is higher than that of P3/4HB/PBS blend. The difference in $t_{0.5}$ becomes more apparent with the increase of crystallization temperature. The results are consistent with the trend of k as listed in Table II. The tiny difference between the calculated half-crystallization time $\tau_{0.5}$ and predicted half-crystallization time $t_{0.5}$ indicated the goodness of the fit close to 50% conversion. All the aforementioned results can lead us to a conclusion that the addition of P3/4HB changes the overall crystallization process of PBS, and increase the crystallization rate of PBS component in the P3/4HB/PBS blends. The higher crystallization rate would be helpful in the processing of the polymer materials.

Mechanical properties of P3/4HB/PBS

The elongation at break, tensile strength, and Young's modulus of P3/4HB and P3/4HB/PBS blends are shown in Table III. When PBS exceeded

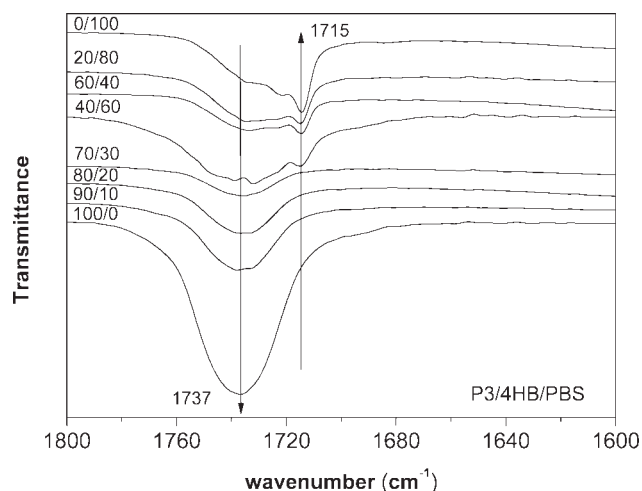


Figure 6 FTIR spectra of carbonyl stretching band region of neat P3/4HB, neat PBS, and P3/4HB/PBS blends.

50 wt %, the blends were too brittle and cracked. No suitable film was prepared by solvent-casting. Therefore, no mechanical data were detected for the blend of more than 50 wt % PBS content. With the PBS content less than 50%, the mechanical properties were determined (Table III). It was noticed that with the addition of PBS, the properties of P3/4HB materials were improved obviously. With the increase of PBS content, the Young's modulus of the blends increase progressively from 53.9 MPa of neat P3/4HB to 197.4 MPa at 40% PBS content. Generally, when the PBS content is less than 30 wt %, the blends possess much improved mechanical properties. The tensile strength and elongation at break gave the maximal value at composition of the PBS 5–10 wt % content. At this point, the P3/4HB/PBS blend has a tensile strength of 16.3–18.0 MPa and elongation at break of 1400%. The Young's modulus

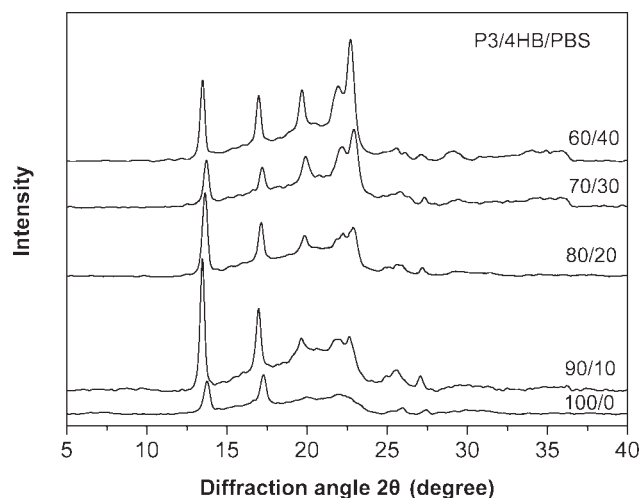


Figure 7 WAXD patterns of the P3/4HB/PBS blends as well as neat P3/4HB.

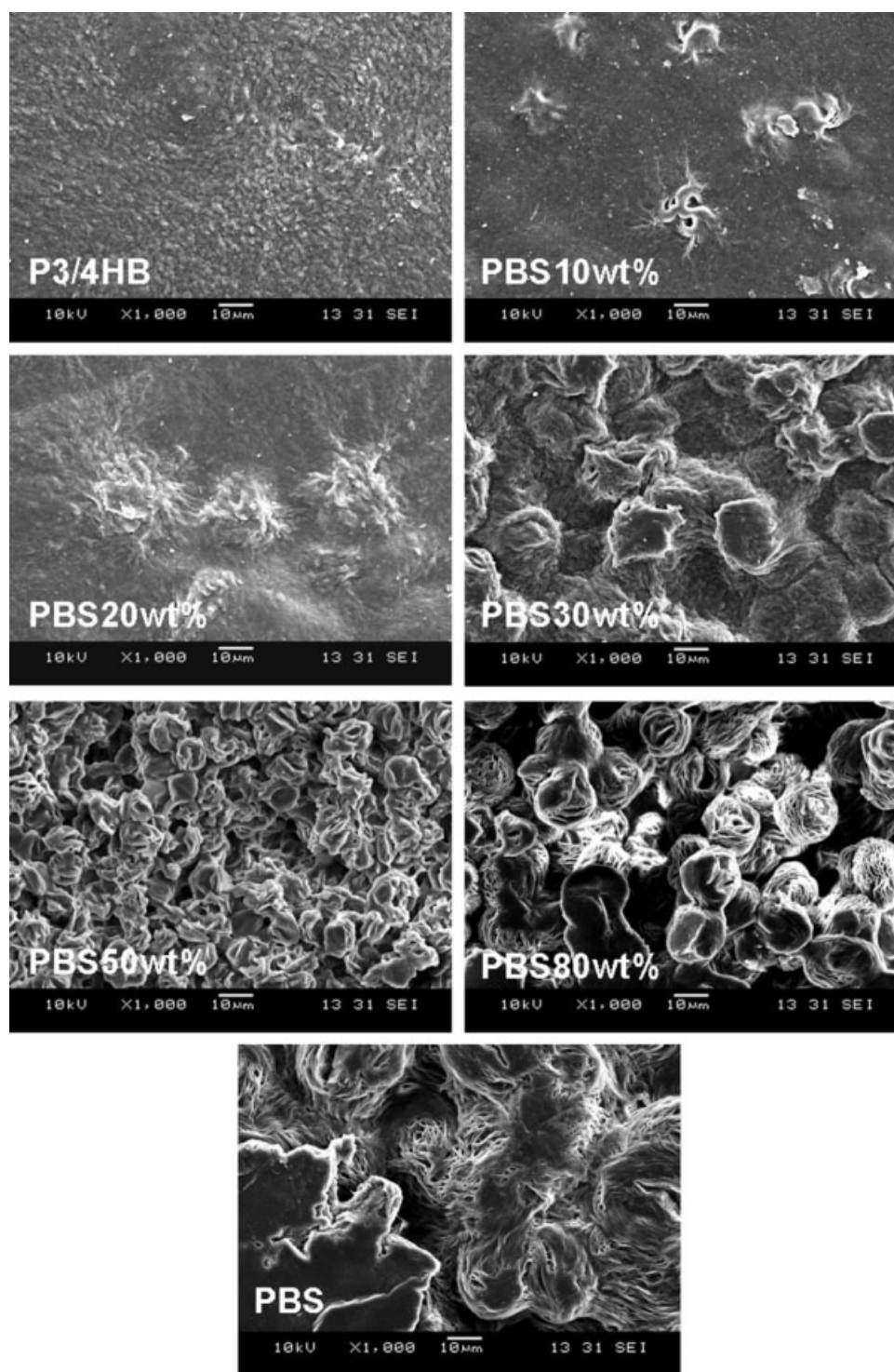


Figure 8 The surface morphology of neat P3/4HB, neat PBS, and their blends.

is, however, still in the range of 51.8–85.3 MPa. Compared with the mechanical properties of neat P3/4HB, the tensile strength and elongation at break of the blends were increased up to 60–80% and 20%, respectively. All these properties demonstrate that the blend is a very good elastic material, which would have wide applications in thermoplastic elastomer industries. But, when the PBS content is

30 wt % and more, the blend shows the poor mechanical properties, with tensile strength of 4.0–7.8 MPa and elongation at break 17.5–77.4%. The mechanical property change is actually consistent with the miscibility difference in the blend system. As we discussed in the miscibility discussion, when PBS content is less than 30 wt %, the P3/4HB/PBS blend possesses better miscibility and thus reveal

higher mechanical properties. On the other hand, when the PBS content is more than 30 wt %, the P3/4HB/PBS blends have lower miscibility and this induces the poor mechanical properties for the system.

FTIR study of P3/4HB/PBS blend

Generally, FTIR was sensitive to conformational and local molecular environment of polymers. It has been extensively used as a convenient and powerful tool for investigating the weak interaction between polymer chains. The strong C=O stretching vibration of neat P3/4HB, PBS, and the blends are shown in Figure 6. The bands at 1737 cm^{-1} and 1714 cm^{-1} were assigned to C=O stretching vibration of neat P3/4HB and neat PBS, respectively. In the P3/4HB/PBS blends, a new shoulder peak at 1732 cm^{-1} was, however, appeared, which should be induced from the C=O absorption shift of the P3/4HB component. This indicates the weak hydrogen bond interaction possibly existed in the P3/4HB/PBS blend system.²⁷

Wide angle x-ray diffraction and crystal structures of the blends

Figure 7 shows the wide-angle X-ray diffraction patterns at ambient temperature for the P3/4HB/PBS blends and P3/4HB. It was observed that the PBS and P3/4HB showed distinct WAXD patterns. The semicrystalline PBS has characteristic X-ray diffraction peaks at $2\theta = 19.6$ and 22.6° ,²⁸ whereas those of the P3/4HB homopolymer were detected at $2\theta = 13.7$ and 17.1° . All of the blends samples clearly showed the same X-ray diffraction peaks at 13.7 , 17.1 , 19.6 , and 22.6° , the characteristic of PBS and P3/4HB crystallites. This result unambiguously demonstrated that the PBS and P3/4HB blends still formed corresponding PBS and P3/4HB type of crystal structures. In addition, the diffraction intensities varied concurrently with the miscibility and weight ratio of P3/4HB/PBS blends, and a similar tendency was detected by the above DSC analysis. Especially, the diffraction intensities at $2\theta = 13.7^\circ$ and 17.1° of the sample P3/4HB/PBS (90/10) were much higher than that of the neat P3/4HB, that suggested the increase of crystallinity of P3/4HB. Those results confirmed that the addition of PBS would enhance the crystallization of P3/4HB. And it also supported the cold crystallization at $40\text{--}60^\circ\text{C}$ in the DSC second heating run was belonged to P3/4HB.

SEM study of P3/4HB/PBS blend

Figure 8 shows the surface morphology of neat P3/4HB, neat PBS, and their blends. When PBS content is less than 30 wt %, the blends films showed typically isolated island structure of PBS domain. P3/

4HB filled in the interspace of PBS as the continuous phase. When PBS content is more than 30 wt %, phase inversion happened. P3/4HB became to be dispersed phase and the interspace of the rigid PBS domains could not be filled completely. The films contained many defects, which would lead to the poor mechanical properties.

CONCLUSIONS

The P3/4HB/PBS blend system possesses varied miscibility depending on the composition. The crystallization rate and degree of PBS and P3/4HB components were enhanced in the blends, compared with neat PBS and neat P3/4HB. The amorphous P3/4HB component would provide more free space to enhance the crystallization of PBS and the PBS would enhance the crystallization of P3/4HB as nucleating agent. The overall isothermal crystallization kinetics of neat PBS and P3/4HB/PBS blends was analyzed by the Avrami equation. The Avrami exponent n of the range from 2.1 to 2.7 was detected, which increases with the crystallization temperature or with the addition of amorphous P3/4HB component. This suggests that the primary crystallization processes should correspond from a two-dimensional circular diffusion-controlled growth geometry and homogeneous nucleation to a three-dimensional spherical growth in the blend system. When PBS content is less than 30 wt %, P3/4HB is the continuous phase and PBS is the isolated island domain. The blends show better miscibility and hence better mechanical properties. When PBS content is more than 30 wt %, the phase inversion happened. The blends have poor miscibility and weaker mechanical properties. The thermal stability of P3/4HB was profoundly enhanced when blended with PBS.

The authors express their sincere gratitude to Li Kang Shi Foundation, for the financial support. Natural Science Foundation of China (NSFC) and National High Tech 863 Grant are also acknowledged.

References

1. Xu, K. T.; Zhao, S. J. *Chin J Appl Environ Biol* 1995, 1, 86.
2. Doi, Y.; Kunioka, M.; Nakamura, Y.; Soea, K. *Macromolecules* 1988, 21, 2722.
3. Doi, Y.; Segawa, A.; Kunioka, M. *Int J Biol Macromol* 1990, 12, 106.
4. Kunioka, M.; Tamaki, A.; Doi, Y. *Macromolecules* 1989, 22, 694.
5. Avella, M.; Martuscelli, E.; Raimo, M. *J Mar Sci* 2000, 35, 523.
6. Li, Q. Y.; Chen, S. T.; Li, Z. B.; Chen, G. Q.; Xu, K. T. *J Biomed Mater Res: Part A*, to appear.
7. Wu, L. P.; Chen, S. T.; Li, Z. B.; Xu, K. T.; Chen, G. Q. *Polym Int* 2008, 57, 939.
8. Wang, L.; Zhu, W. F.; Wang, X. J.; Chen, X. Y.; Chen, G. Q.; Xu, K. T. *J Appl Polym Sci* 2008, 107, 166.

9. Xu, S. L.; Luo, R. C.; Wu, L. P.; Xu, K. T.; Chen, G. Q. *J Appl Polym Sci* 2006, 102, 3782.
10. Chatani, Y.; Hasegawa, R.; Tadokoro, H. *Polym Prepr Jpn* 1971, 20, 420.
11. Ihn, K. J.; Yoo, E. S.; Im, S. S. *Macromolecules* 1995, 28, 2460.
12. Ichikawa, Y.; Suzuki, J.; Washiyama, J.; Moteki, Y.; Noguchi, K.; Okuyama, K. *Polymer* 1994, 35, 3338.
13. Ichikawa, Y.; Kondo, H.; Igarashi, Y.; Noguchi, K.; Okuyama, K.; Washiyama, J. *Polymer* 2000, 41, 4719.
14. Yoo, E. S.; Im, S. S. *J Polym Sci Polym Phys* 1999, 37, 1357.
15. Miyata, T.; Masuko, T. *Polymer* 1998, 39, 1399.
16. Gan, Z.; Abe, H.; Kurokawa, H.; Doi, Y. *Biomacromolecules* 2001, 2, 605.
17. Qiu, Z. B.; Fujinami, S.; Komura, M.; Nakajima, K.; Ikehara, T.; Nishi, T. *Polym J* 2004, 36, 642.
18. Qiu, Z. B.; Komura, M.; Ikehara, T.; Nishi, T. *Polymer* 2003, 44, 7781.
19. Lee, J. C.; Tazawa, H.; Ikehara, T.; Nishi, T. *Polym J* 1998, 30, 327.
20. Lee, J. C.; Tazawa, H.; Ikehara, T.; Nishi, T. *Polym J* 1998, 30, 780.
21. Qiu, Z. B.; Ikehara, T.; Nishi, T. *Polymer* 2003, 44, 2799.
22. Qiu, Z. B.; Ikehara, T.; Nishi, T. *Polymer* 2003, 44, 3095.
23. Qiu, Z. B.; Ikehara, T.; Nishi, T. *Polymer* 2003, 44, 2503.
24. Qiu, Z. B.; Ikehara, T.; Nishi, T. *Polymer* 2003, 44, 7519.
25. Lorenzo, A. T.; Arnal, M. L.; Albuérne, J. *Polym Test* 2007, 26, 222.
26. Wunderlich, B. *Macromolecular Physics*; Academic: New York, 1977; Vol. 2.
27. Barham, P.; Keller, A. J.; Otun, E. L.; Holmes, P. A. *J Mater Sci* 1984, 19, 2781.
28. Ba, C. Y.; Yang, J.; Hao, Q. H.; Liu, X. Y.; Cao, A. *Biomacromolecules* 2003, 4, 1827.